7. Shaw T, Smillie RH, MacPhee DG. The role of blood platelets in nucleoside metabolism: assay, cellular location and significance of thymidine phosphorylase in human blood. *Mutat Res* 1988;200:99–116.
8. Usuki K, Norberg L, Larsson E, et al. Localization of platelet-derived endothelial cell growth factor in human placenta and purification of an alternatively processed form. *Cell Regulation* 1990;1:577–596.
9. Graham MM, Lewellen BL. High-speed automated discrete blood sampling for positron emission tomography. *J Nucl Med* 1993;34:1357–1360.
10. Shields AF, Lim K, Grierson J, Link J, Krohn KA. Utilization of labeled thymidine in DNA synthesis: studies for PET. *J Nucl Med* 1990;31:337–342.
11. Shields AF, Graham MM, Kozawa SM, et al. Contribution of labeled carbon dioxide to PET imaging of carbon-11-labeled compounds. *J Nucl Med* 1992;33:581–584.
12. Cleaver JE. Thymidine metabolism and cell kinetics. *Frontiers Biol* 1967;6:43–100.
13. Nottebrock H, Then R. Thymidine concentrations in serum and urine of different animal species and man. *Biochem Pharmacol* 1977;26:2175–2179.
14. Vander Borght TM, Lambotte LE, Pauwels SA, Dive CC. Uptake of thymidine labeled on carbon 2: a potential indicator of liver regeneration by positron emission tomography. *Hepatology* 1990;12:113–118.
15. Quackenbush RC, Shields AF. Local re-utilization of thymidine in normal mouse tissues as measured with iododeoxyuridine. *Cell Tissue Kinetics* 1988;21:381–387.
16. Shields AF, Coonrod DV, Quackenbush RC, Crowley JJ. Cellular sources of thymidine nucleotides: Studies for PET. *J Nucl Med* 1987;28:1435–1440.
17. Mankoff DA, Shields AF, Lee TT, Graham MM. Tracer kinetic model for quantitative imaging of thymidine utilization using ^{11}C-thymidine and PET [Abstract]. *J Nucl Med* 1994;35:138P.
18. Graham MM. Parameter optimization programs for positron emission tomography data analysis. *Ann Nucl Med* 1993;7:S42–S43.
19. Press WH, Flannery BP, Teukolsky SA, Vetterling WT. *Numerical recipes in Pascal: the art of scientific programming*. New York: Cambridge University Press; 1989. 572–580.

FDG-PET Evaluation of Therapeutic Effects on VX2 Liver Tumor

Natsuo Oya, Yasushi Nagata, Nagara Tamaki, Takehisa Takagi, Rumi Murata, Yasuhiro Magata, Mitsuyuki Abe and Junji Konishi
Departments of Radiology and Nuclear Medicine, Faculty of Medicine, Kyoto University, Kyoto, Japan

Transplanted VX2 liver tumor in the rabbit is an experimental liver tumor model in which ^{18}F-2-fluoro-2-deoxy-D-glucose (FDG) accumulates to a 3.5-fold level that surrounds normal liver tissue. In this study, changes in FDG uptake were assessed in this liver tumor model after transcatheter arterial embolization (TAE) and radiotherapy. **Methods:** Fifteen rabbits bearing VX2 liver tumors were treated with TAE with gelatin sponges 1 day before the FDG study, and 18 rabbits received local irradiation with electron beams at a dose of 12–36 Gy 1–10 days before the FDG study. In the FDG study, serial arterial blood sampling was performed to determine arterial input (AI), and 1 hr after tracer injection, normal liver tissue and tumor tissue were excised to measure radioactivity. The tumor FDG level per AI and the tumor-to-normal liver ratio were assessed. Dynamic PET images were obtained in 20 of the 46 rabbits. **Results:** Tumor FDG uptake was significantly decreased 1 day after TAE (from 3.54 to 0.83 in the tumor-to-normal liver ratio) and 5 days after 30 Gy of irradiation (from 3.54 to 1.28). The decrease in tumor FDG uptake was dose-dependent, especially in the relatively low dose range (12–24 Gy). The untreated tumors could be clearly distinguished from the surrounding normal liver tissue, while the embolized tumors or the irradiated tumors were not clearly delineated. Histological analysis showed that the decrease in tumor FDG after treatment agreed well with the decrease in number of viable tumor cells. **Conclusion:** The VX2 liver tumor is an appropriate experimental tumor model for evaluating the change in FDG uptake in various therapeutic modalities. Moreover, the therapeutic effects can be assessed 1 day after TAE and 5 days after irradiation. Further clinical trials for the early evaluation of therapeutic effects on liver tumors using FDG-PET are warranted.

Key Words: fluorine-18-fluorodeoxyglucose; VX2 tumor; transcatheter arterial embolization; radiotherapy

J Nucl Med 1996; 37:296–302

Many experimental and clinical studies have shown increased uptake of ^{18}F-2-fluoro-2-deoxy-D-glucose (FDG) in malignant tumors with increased glucose utilization (*1–7*). In terms of clinical use, metabolic imaging of tumors by FDG-PET is useful in differentiating malignant tumor from benign disease (*8–10*), assessing the degree of differentiation (*11–15*) and detecting recurrences (*10,16*). In addition, several studies have suggested the usefulness of FDG-PET for evaluating therapeutic effects. Most of these clinical studies indicated that FDG uptake in tumors decreases after radiotherapy (*17–22*), chemotherapy (*18*) and transcatheter arterial embolization (TAE) (*23*). Some of these studies suggest that the prognosis could be predicted by the decrease in tumor FDG uptake (*18,21,22*).

Also, decreased FDG uptake following radiotherapy or chemotherapy has been demonstrated in mouse and rat experimental tumor models (*24–27*). Transplanted VX2 tumor in the rabbit is an experimental tumor model in which FDG accumulates to levels several-fold those in normal organs (*2–4*). In our previous study, VX2 tumors transplanted in the rabbit liver were evaluated by FDG-PET (*5*). In the present study, the change in FDG uptake in the transplanted VX2 liver tumor was assessed after TAE and radiotherapy to determine the usefulness of FDG-PET in this model for evaluating the effects of therapy.

MATERIALS AND METHODS

Animals and Tumors

Male Japanese white rabbits (weighing 2–4 kg) were used in this study. Rabbits were anesthetized with 25 mg/kg b.w. sodium pentobarbital, and a midline abdominal incision was made. Two-to-six blocks of VX2 tumor tissue containing approximately 4–10 $\times 10^5$ VX2 cells were transplanted directly into each rabbit's liver (*5,28*). Forty-six rabbits with VX2 liver tumors over 2 cm in diameter 3–4 wk after transplantation were used in the following experiments. Twenty-one of these rabbits had multiple liver tumors and/or nonhepatic tumors (e.g., tumors in overlying muscular layer or peritoneum).

FDG

Fluorine-18 was produced by the ^{20}Ne(d, α)^{18}F nuclear reaction using an ultracompact cyclotron. Fluorine-18-FDG was then synthesized by the acetylhypofluorite method of Shiue et al. (*29*) with slight modifications. The specific activity of the [^{18}F]FDG thus obtained was 143 to 204 MBq/mg and the radiochemical purity was over 95% as assessed by HPLC (eluent, CH_3CN:H_2O = 85:15).

Received Dec. 27, 1994; revision accepted Jul. 29, 1995.
For correspondence or reprints contact: Natsuo Oya, MD, Department of Radiology, Kyoto University Hospital, 54 Kawahara-cho, Shogoin, Sakyo-ku, Kyoto 606, Japan.

TAE and Radiotherapy

Fifteen rabbits were treated with TAE using gelatin sponges 1 day before the FDG study (TAE group). The rabbits bearing VX2 liver tumors were anesthetized with sodium pentobarbital and a 4-Fr angiographic catheter was inserted through the exposed right femoral artery. The proper hepatic artery was then selectively catheterized under fluoroscopic guidance. The proper hepatic artery was embolized with the gelatin sponge (approximately 0.5 mm in diameter)/Iopamiron® 300 (Bracco, Italy) suspension. Injection of the suspension was completed when blood flow interruption was confirmed (*28,30*).

Eighteen rabbits received local irradiation with electron beams at a single fraction of 12–36 Gy and 1–10 days before the FDG study (RT group). They were divided into six subgroups (12 Gy 10 days, 24 Gy 10 days, 30 Gy 10 days, 36 Gy 10 days, 30 Gy 1 day, and 30 Gy 5 days), each consisting of three rabbits. A small abdominal incision was made under general anesthesia to allow the tumor palpation. Then, a circular irradiation field 4 cm in diameter was determined so that at least one of the liver tumors should be included. In all cases, the liver tumors were irradiated with 6 MeV external electron beam generated using a linear accelerator at a dose rate of 3 Gy/min. Thirteen rabbits were not treated (control group).

FDG Study

In the FDG study, tumor-bearing rabbits were anesthetized after 4 hr of fasting with sodium pentobarbital. Then the rabbits received an intravenous injection of 1–54 MBq/kg body weight (b.w.) of [^{18}F]FDG through an auricular vein over a 30-sec period; the time of commencement of injection was defined as time 0.

Arterial blood sampling and tissue excision were performed in all 46 rabbits (15 of the TAE group, 18 of the RT group and 13 of the control group), according to the previous study (*5*). Briefly, 14 serial arterial blood samples were obtained over a 60-min period from a catheter introduced into the femoral artery following [^{18}F]FDG injection. The ^{18}F level in the collected plasma was measured with an automated NaI well scintillation counter to determine the arterial input (AI). Immediately after the last arterial blood sample was obtained (i.e., time 60 min), each rabbit was killed with a lethal dose of pentobarbital, and a number of small pieces (up to 0.7 g) of tumor tissue and normal liver were excised. The ^{18}F level in the excised tissue specimens was then measured. Central necrotic tissue in the tumor was carefully and strictly removed using fingers or forceps. The normal liver tissue around the tumor could be easily removed with scissors.

Dynamic PET images were obtained with an animal PET camera in 20 rabbits (5 of the TAE group, 7 of the RT group, and 8 of the control group). Each anesthetized rabbit was fixed in the gantry of the camera and a transmission scan was obtained for 15 min with a ^{68}Ge ring. Sequential 3-min scans were performed over the 60-min period following 7–54 MBq/kg b.w. [^{18}F]FDG injection. The transaxial and axial resolution of the system were 3.0 mm and 4.8 mm (FWHM), respectively, at the center of the field of view. The slice aperture was 8 mm, and the averaged direct slice sensitivity and cross-slice sensitivity were 2.3 kcps/μCi/ml and 3.8 kcps/μCi/ml, respectively. Total system sensitivity was 20.7 kcps/μCi/ml, including the scatter component (*31*). The procedure is summarized in Figure 1.

Data Analysis

For all 46 rabbits, the plasma ^{18}F level (Cp(t)) was determined as a function of time following [^{18}F]FDG injection. AI was determined as the area under the curve of Cp(t) for 60 min.

Fluorine-18 level in the excised VX2 tumor tissue (Cv) and in the excised normal liver tissue (Cl) were also determined for all rabbits. Ten of 15 rabbits of the TAE group had not only hepatic

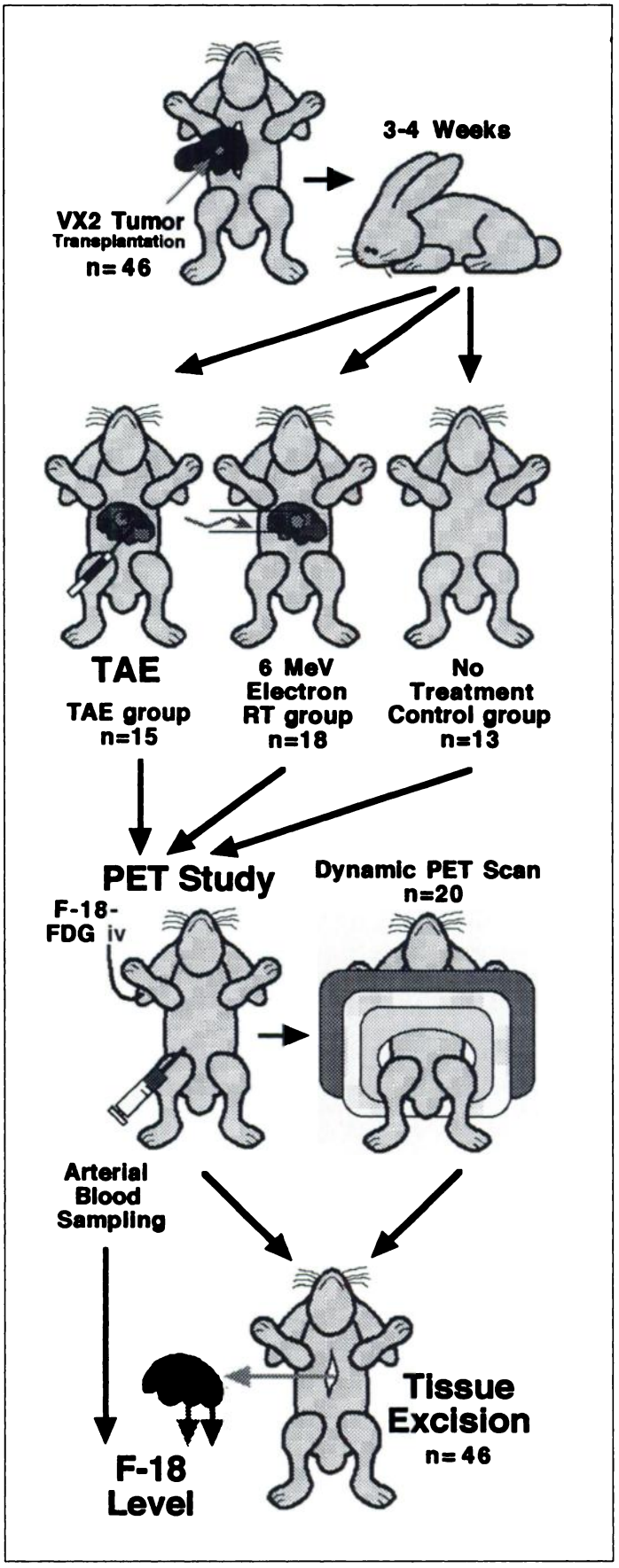

FIGURE 1. Summary of methods.

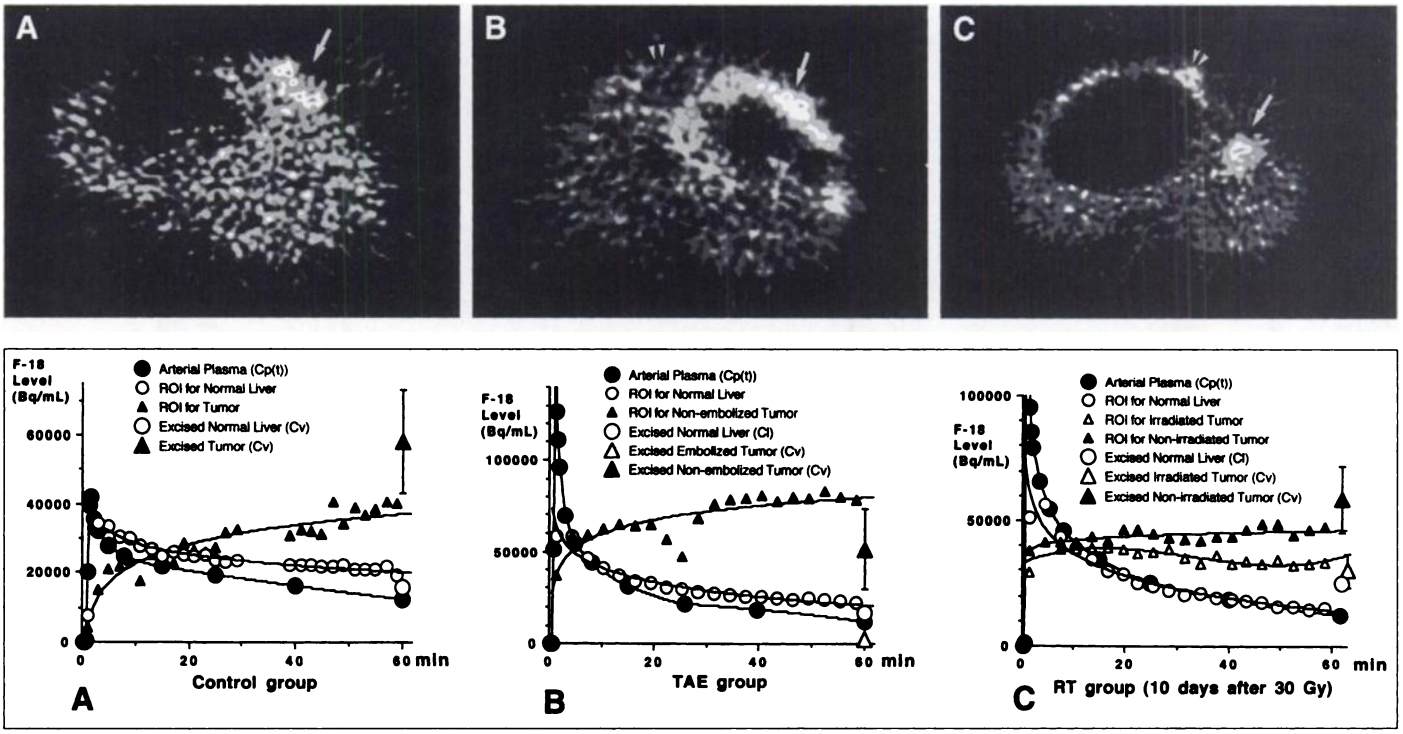

FIGURE 2. PET images obtained in the last 3-min scan (top panels: A–C) and time-activity curves (bottom panels: A–C) of a rabbit representing the control, TAE and RT groups. The VX2 liver tumor in the control group, the nonembolized tumor on the abdominal wall in the TAE group and the nonirradiated tumor in the RT group were clearly distinguishable (arrows). The embolized tumor in the TAE group was not delineated, and the irradiated tumor in the RT group was less clearly distinguished from surrounding normal liver tissue (paired arrowheads). Error bars are 1 s.d. from 3–6 specimens.

tumors but also nonhepatic tumors (e.g., tumors in overlying muscular layer or peritoneum). Since nonhepatic tumors were fed mainly by arteries other than the hepatic artery, they were regarded to be nonembolized tumors. Cv was assessed separately for the nonembolized tumors (i.e., nonhepatic tumors) and the embolized tumors (i.e., hepatic tumors). Eleven of 18 rabbits of the RT group also had tumors out of the irradiation fields, which were regarded to be nonirradiated tumors. Cv was assessed separately for the nonirradiated tumors (i.e., tumors out of the irradiation field) and the irradiated tumors (i.e., tumors within the irradiation field).

For the tumors in the rabbits investigated by dynamic PET imaging, the graphical method was used to determine the K-complex (K), according to previous reports (*5,32,33*). Briefly, K was determined as the slope of the linear portion of the graph obtained by plotting Cv(t)/Cp(t) versus $\int_0^t Cp(\tau)d\tau/Cp(t)$, where Cv(t) is ^{18}F level in the ROI drawn for the tumor at time t. K was determined for the control tumors, the nonembolized tumors in the TAE group and the nonirradiated tumors in the RT group. K for the irradiated tumors was also determined, whenever regions of interest (ROIs) could be drawn for the irradiated tumors.

Cl/AI, Cv/AI, Cv/Cl (i.e., tumor-to-normal liver ratio) and K were compared among the three groups. Student's t-test was used for statistical analysis.

RESULTS

FDG Study

The plasma glucose level ranged from 96 to 252 (150 ± 38, mean ± s.d.) mg/dl, which correlated with neither Cl/AI nor Cv/AI. AI varied with the dose of [^{18}F]FDG and ranged from 1.4×10^4 to 7.1×10^6 (1.1×10^6, median) (Bq/ml) × min.

Figure 2 shows the representative PET images obtained in the last 3-min scan and time-activity curves of the three groups. In the images, all the tumors in the control group, the nonembolized tumors in the TAE group and the nonirradiated tumors in the RT group could be clearly distinguished from the surrounding normal liver tissue. Dynamic PET images were obtained in 7 of 18 rabbits in the RT group and 6 of the 7 irradiated tumors were distinguishable, 5 of which showed lower uptake than the tumors in the control group. Dynamic PET images were obtained in 5 of 15 rabbits in the TAE group, and none of the 5 embolized tumors could be clearly described in the images. ROIs were drawn for the normal liver in all cases and for the tumors if distinguishable, and serial changes of the ^{18}F level in the ROI were plotted versus time. Following [^{18}F]FDG injection, the ^{18}F level in the ROIs for the VX2 liver tumor gradually increased, whereas that for the normal liver decreased almost in parallel to the ^{18}F level of arterial plasma (Cp(t)).

Cl/AI, Cv/AI, Cv/Cl, K and tumor weight are compared among the three groups in Table 1. Cl/AI did not differ among the three groups. Normal liver treated with TAE was not damaged because of the blood supply from the portal vein. Normal liver irradiated under the present experimental conditions (within 10 days after irradiation of up to 36 Gy) also showed no significant change in respect of FDG uptake. Cv/AI in the control group was approximately 3.5-fold higher than Cl/AI, corresponding with the clear tumor description against the surrounding normal liver tissue. Cv/AI for the embolized tumors decreased significantly within 1 day after TAE. Since Cv/AI was similar to Cl/AI, accurate ROI could not be determined for the embolized tumor, nor could K. Ten days after irradiation, Cv/AI for the irradiated tumors decreased dose-dependently at least up to 36 Gy which was the maximal dose examined. Cv/AI at a dose of 30 Gy was variable 1 day after irradiation, and decreased significantly 5 and 10 days after irradiation. Generally, Cv/AI for the irradiated tumors was considerably higher than that for the embolized tumors. So, in six cases of the RT group, ROI also could be determined for the irradiated tumor, so could K. K was decreased significantly 5 days after irradiation with 30 Gy. Both the nonembolized and nonirradiated tumors were described clearly in the obtained

TABLE 1
Summary of the Results

	Treatment	No. of assessed tumors	Cl/AI (min^{-1})*	Cv/AI (min^{-1})*	Cv/Cl*	K (min^{-1})	Tumor weight† (g)*
Control group (n = 13)	None	13	0.0131 ± 0.0026	0.0441 ± 0.0088	3.54 ± 0.88	0.0341 ± 0.0059*	4.1 ± 1.8
TAE group (n = 15)	No embolization	10	—	0.0350 ± 0.0114‡	2.65 ± 0.96‡	0.0252 ± 0.0160*	—
	Embolization	15	0.0139 ± 0.0051	0.0113 ± 0.0070§	0.83 ± 0.48§	—	3.8 ± 2.0
RT group (n = 18)	No irradiation	11	—	0.0313 ± 0.0080§	2.80 ± 0.81‡	0.0185 ± 0.0040*§	—
	10 days after 12 Gy	3	0.0116 ± 0.0025	0.0217 ± 0.0121§	1.80 ± 0.55‡	—	3.1 ± 0.8
	10 days after 24 Gy	3	0.0125 ± 0.0013	0.0189 ± 0.0052§	1.33 ± 0.42§	—	4.2 ± 1.8
	10 days after 30 Gy	3	0.0130 ± 0.0011	0.0170 ± 0.0008§	1.32 ± 0.14§	0.0120¶	3.6 ± 1.8
	10 days after 36 Gy	3	0.0116 ± 0.0008	0.0154 ± 0.0003§	1.40 ± 0.01§	0.0111¶	3.9 ± 2.3
	1 day after 30 Gy	3	0.0102 ± 0.0020	0.0322 ± 0.0132	3.28 ± 1.49	0.0621¶	3.6 ± 0.4
	5 days after 30 Gy	3	0.0110 ± 0.0002	0.0140 ± 0.0013§	1.28 ± 0.10§	0.0077 ± 0.0043*§	4.3 ± 2.5

*Mean ± s.d.
†Weight of the solid part of tumor.
‡§Significantly lower than the control in the respective columns (‡$p < 0.05$; §$p < 0.005$).
¶Only one tumor was assessed.

images. Cv/AI for these tumors were significantly, although only a little, lower than Cv/AI in the control group.

Histological Study

Photomicrographs of a tumor in the control group, an embolized tumor in the TAE group and an irradiated tumor in the RT group are shown in Figure 3. The untreated tumor consisted of viable VX2 cells with bright and large nuclei (Fig. 3A). The mitotic index was about 0.5%. Inflammatory cell infiltration was rarely seen. In the tumor treated with TAE, degenerated tumor cells with nuclear condensation, localized hemorrhage and macrophage infiltration around the cell debris were observed (Fig. 3B). Viable tumor cells were rarely seen. In the tumor excised on the 10th day after irradiation at a dose of 30 Gy, the number of viable VX2 cells was markedly decreased, and they were replaced by the fibrous tissue. Localized eosinophil infiltration was also observed (Fig. 3C).

DISCUSSION

Our findings indicate that transplanted VX2 liver tumor is an appropriate model for evaluating changes in FDG uptake evolved by TAE and radiation therapy. A decrease in FDG uptake was observed on 1 day after TAE and 5 days after irradiation. Furthermore, such decreases were associated with decreases in the number of viable cells as determined by histological examination.

Previous Studies of FDG-PET after TAE

Some clinical studies have indicated that imaging of tumors by FDG-PET is useful for evaluating the effects of TAE. For instance, Nagata et al. studied FDG-PET in patients with malignant liver tumors several weeks after TAE and demonstrated its usefulness for monitoring the efficacy of treatment (*23*). Torizuka et al. compared the FDG-PET and histological examination of hepatocellular carcinoma 3–45 days after TAE, suggesting that the tumors with decreased or absent FDG uptake were highly necrotic (*34*). Since malignant liver tumors are often treated with TAE, the value of FDG-PET for evaluating the therapeutic effects of this treatment should be tested experimentally.

Decreased Cell Number after TAE

In the present study, a marked decrease in FDG uptake was observed in the VX2 liver tumor model even 1 day after TAE, suggesting the usefulness of FDG-PET for early evaluation of the therapeutic effects of this treatment. Even in the control group, large VX2 tumors tended to show spontaneous central necrosis. In the present study, almost all tumors over 3 cm in diameter were accompanied with spontaneous central necrosis. This was often included in the ROIs, but usually excluded from excised tumor specimens for radioactivity counting. Therefore, FDG uptake in the excised tumor did not depend on tumor size or the degree of spontaneous necrosis. In the TAE group, the proportion of the central necrosis in the embolized tumor seemed to have been increased, but it should be noted again that the cell debris had been removed before radioactivity counting. Thus, the decreased Cv/AI corresponded to the decreased FDG uptake in the solid part of the tumor. Histological analysis showed a marked decrease in the number of vivid tumor cells, replacement by degenerated cells and persistent cell debris even in the solid part of the tumors. Thus, there is no doubt that the rapid decrease in FDG uptake in the embolized tumor can be explained by the decrease in the number of viable cells. Large numbers of tumor cells seemed to have been killed within 1 day after TAE by acute environmental changes such as anoxia and nutrient deficiency induced by TAE. Of course, some viable tumor cells might have survived and a number of macrophages had infiltrated, but their proportion to the whole tumor seemed to be too small to elevate tumor FDG uptake significantly.

Decreased FDG Input after TAE

As another interpretation on the decreased FDG uptake, it is also probable that the interruption of arterial blood flow reduced the FDG input to the embolized tumor during the 1 hr following FDG injection. The tumor FDG input must have been smaller than AI, which was determined by blood sampling from the femoral artery, and the reduced FDG input to the surviving tumor cells might result in underestimation of tumor FDG uptake. It seems, however, that this reduced tumor FDG input did not play an important role in the decrease in tumor FDG uptake. The surviving tumor cells must have been provided with glucose by a certain pathway (e.g., perfusion from surrounding liver) to survive for 1 day following TAE. Consequently, they should have necessarily had a chance to also incorporate injected FDG during 1 hr of the study through the same pathway for glucose uptake. The period of 1 hr seems to be long enough for a considerable part of injected FDG to reach the tumor by perfusion from the surrounding liver.

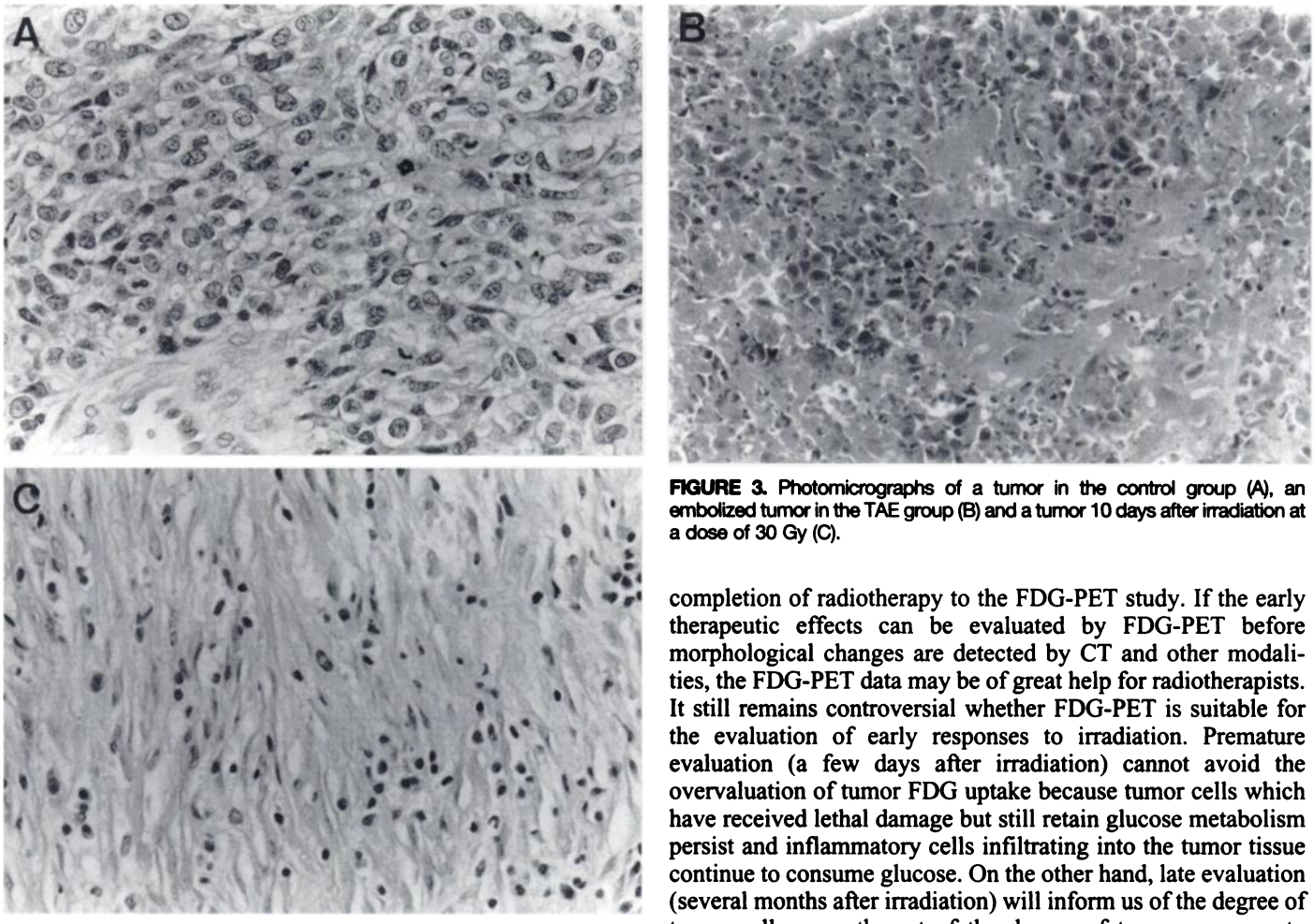

FIGURE 3. Photomicrographs of a tumor in the control group (A), an embolized tumor in the TAE group (B) and a tumor 10 days after irradiation at a dose of 30 Gy (C).

Nonembolized Tumor in the TAE Group

Cv/AI for the nonembolized tumors in the TAE group was slightly lower than Cv/AI in the control group. This was probably because some of the nonembolized tumors were fed partly by the proper hepatic artery, or because general malnutrition might have been induced by the stress of TAE.

Previous Clinical Studies of FDG PET after Irradiation

Many clinical studies have demonstrated the usefulness of FDG-PET for the evaluation of radiation therapy, suggesting a correlation between the decrement of tumor FDG uptake after radiation therapy and the local response (*17,18*) and differentiating tumor recurrence from radiation necrosis (*10,21*). Several clinical studies have also indicated that tumor FDG uptake does not necessarily decrease or may even increase after irradiation despite good tumor response in clinical evaluation. For example, Rozental et al. (*35*) showed an increase in glucose uptake ratio in metastatic and primary brain tumor 1 day after stereotactic radiotherapy. Okada et al. (*20*) reported that non-Hodgkin's lymphoma successfully treated with chemotherapy and radiotherapy often showed high FDG uptake when assessed 1–8 days after treatment. Haberkorn et al. (*19*) studied patients with recurrent colorectal carcinoma and showed that the decrease in FDG uptake even 6 wk after therapy was not satisfactory in half of the patients with good local response (*19*). In these reports, the positive FDG-PET study after clinically successful radiotherapy was explained mainly by the inflammatory reaction induced by radiation. They recommend the evaluation by FDG-PET over 3–6 mo after irradiation to exclude completely the influence of inflammation (*19*).

It is a major problem to determine the optimal interval from completion of radiotherapy to the FDG-PET study. If the early therapeutic effects can be evaluated by FDG-PET before morphological changes are detected by CT and other modalities, the FDG-PET data may be of great help for radiotherapists. It still remains controversial whether FDG-PET is suitable for the evaluation of early responses to irradiation. Premature evaluation (a few days after irradiation) cannot avoid the overvaluation of tumor FDG uptake because tumor cells which have received lethal damage but still retain glucose metabolism persist and inflammatory cells infiltrating into the tumor tissue continue to consume glucose. On the other hand, late evaluation (several months after irradiation) will inform us of the degree of tumor cell regrowth, not of the degree of tumor response to current radiotherapy.

Previous Laboratory Studies of FDG PET after Irradiation

In laboratory studies, changes in tumor FDG uptake after irradiation have been assessed using rodent tumors. Kubota et al. (*24*) and Abe et al. (*25*) examined the transplanted tumors of the mouse and rat and found that the tumor FDG uptake decreased gradually with time up to 6–8 days following irradiation (*24,25*). It is, however, not clear whether this relatively slow response is due to inflammation or delayed cell death. It has been reported independently that FDG actually accumulates in inflammatory cells as well as malignant tumor cells in FM3A tumor in the mouse (*36*). In addition, FDG and ^{14}C-methionine were compared (*25,37*), and it was suggested that ^{14}C-methionine was superior to FDG for evaluating early effects of irradiation since ^{14}C-methionine showed a more rapid response.

Interval from the Irradiation to FDG-PET

The present experiments showed that the FDG uptake in the VX2 liver tumor was variable on the first day after irradiation with 30 Gy but decreased significantly on the 5th day. A small difference was observed between the 5th and the 10th day. Therefore, it was suggested that, at least for this tumor model, 1 day was too short and 5 days was long enough as an interval from irradiation to FDG analysis. This agreed with the data on other tumor models in rats and mice (*24,25*). Histological analysis showed that the number of viable tumor cells was decreased 10 days after irradiation, which corresponds to the decreased FDG uptake. In the present study, the degree of inflammatory cell infiltration after irradiation was still lower

than that after TAE, suggesting that the inflammatory reaction did not largely affect the tumor FDG uptake after irradiation.

Furthermore, the decrease in FDG uptake in VX2 liver tumor preceded changes in size up to 10 days after irradiation, which suggests the usefulness of FDG-PET in evaluating early effects of irradiation. Although the radiosensitivity of VX2 tumor was not determined in detail, tumor size and degrees of central necrosis 5 and 10 days after 30 Gy irradiation were not significantly different from those of the control tumor. On the other hand, previous studies showed that both FM3A tumor in the mouse and AH109A tumor in the rat decreased in size 5–10 days after irradiation with 20 Gy (*24,25*). Thus, the VX2 tumor seemed to be more radioresistant than these tumors, although the comparison may not be appropriate because these tumors were inoculated subcutaneously and were smaller in size at irradiation. Tumor FDG uptake decreased 5 days after irradiation, while the size of the VX2 tumor did not change up to 10 days after irradiation. Therefore, FDG-PET seemed to have an advantage over CT or other morphological imaging modalities, especially when the therapeutic effect was evaluated 5–10 days after irradiation. Unfortunately, further observation was unsuccessful due to unavoidable pulmonary metastases, which became fatal 5–6 wk after transplantation.

Irradiation Dose-Dependency

Tumor FDG uptake decreased dose-dependently when evaluated 10 days after irradiation. The difference in FDG uptake between 24 and 36 Gy was smaller than that between 12 and 24 Gy. A similar tendency was observed in other tumor models, and ^{14}C-methionine showed more sensitive dose-dependency than FDG (*24,25*). To understand this phenomenon, it is important to know why tumor FDG uptake decreases after irradiation. Higashi et al. (*38*) assessed the FDG uptake in the human cancer cell line in vitro and showed that FDG uptake in the culture was strongly related to the number of viable tumor cells (*38*) and FDG incorporation per single viable cell was not related to the proliferative activity or surviving probability of the irradiated cells (*39*). Thus, decreased FDG uptake after irradiation is due largely to the decreased number of viable cells. FDG can differentiate viable cells from dead cells but cannot differentiate proliferable cells from dying cells, while ^{14}C-methionine (and other markers of protein or DNA synthesis) may correlate well with the proliferative capacities of the viable cells. In the in vivo assessment, tumor FDG uptake is determined only as an average of the whole tumor. The difference in the number of viable tumor cells between 24 and 36 Gy is smaller than that between 12 and 24 Gy. A subtle difference may be missed being involved in the environmental changes such as blood flow, inflammation and other factors in vivo. Therefore, it should be noted that FDG can judge whether the tumor response has been good or not, but it cannot predict whether the tumor will recur. This relatively low sensitivity to detect the differences in effects at higher radiation dose range seems to be a limitation of the FDG-PET.

Nonirradiated Tumor in the RT Group

Cv/AI for the nonirradiated tumors in the RT group was slightly lower than Cv/AI in the control group. Although the tumors to receive no irradiation were strictly excluded from the 4 cm-diameter circle drawn for the irradiation field at the setting, they may possibly have been received a few percent of the irradiated dose because of respiratory movement and/or the lateral expansion of the electron beams.

Clinical Applications

There are several essential differences between the radiotherapy of clinical tumors and that of experimental tumors. First, most clinical tumors, including liver tumors, are usually irradiated by fractionated regimens, in which cell loss and repopulation occur continuously. Under these conditions, a longer interval from the completion of the therapy to the stabilization of the tumor cell kinetics would be required. In addition, the inflammatory reaction would be strong and prolonged due to longer total treatment time. Second, most clinical tumors grow more slowly than this experimental model. A tumor cell population with a longer cell cycle and smaller growth fraction will respond later, if mitotic death is the predominant cause of death (*40*). Third, some clinical tumors have quite small populations of tumor cells in the tumor tissue, a large part of which consists of mainly fibrous tissue. This may result in undervaluation of the therapeutic effects. Despite these differences, we believe that the evaluation of the therapeutic effects on human liver tumors by FDG-PET would be appropriate a few days after TAE and a few weeks after irradiation.

CONCLUSION

The VX2 liver tumor is an appropriate experimental tumor model for evaluating changes in FDG uptake by various therapeutic modalities. The decrease in tumor FDG uptake in this model can be assessed 1 day after TAE and 5 days after irradiation. The decrease in tumor FDG uptake after irradiation correlates with the dose given, especially at relatively low doses and the decrease in tumor FDG after treatment agrees well with the decrease in the number of viable tumor cells. Therefore, further clinical trials for the early evaluation of therapeutic effects on human liver tumors using FDG-PET are warranted.

ACKNOWLEDGMENTS

The authors thank Dr. Masahiro Hiraoka for valuable comments and Hamamatsu Photonics K.K. for developing and supplying the animal PET system.

REFERENCES

1. Som P, Atkins HL, Bandoypadhyay D, et al. A fluorinated glucose analog, 2-fluoro-2-deoxy-D-glucose (^{18}F): nontoxic tracer for rapid tumor detection. *J Nucl Med* 1980;21:670–675.
2. Fukuda H, Matsuzawa T, Abe Y, et al. Experimental study for cancer diagnosis with positron-labeled fluorinated glucose analogs: ^{18}F-2-fluoro-2-deoxy-D-mannose: a new tracer for cancer detection. *Eur J Nucl Med* 1982;7:294–297.
3. Fukuda H, Toshioka S, Watanuki S, et al. Experimental study for cancer diagnosis with ^{18}FDG: differential diagnosis of inflammation from malignant tumor. *Kaku Igaku* 1983;20:1189–1192.
4. Abe Y, Matsuzawa T, Fukuda H, et al. Experimental study for tumor detection using ^{18}F-2-fluoro-2-deoxy-D-glucose: imaging of rabbit VX2 tumor with single photon gamma gamera. *Kaku Igaku* 1985;22:389–391.
5. Oya N, Nagata Y, Ishigaki T, et al. Evaluation of experimental liver tumors using fluorine-18-2-fluoro-2-deoxy-D-glucose PET. *J Nucl Med* 1993;34:2124–2129.
6. Yonekura Y, Benua RS, Brill AB, et al. Increased accumulation of 2-deoxy-2-^{18}F-fluoro-D-glucose in liver metastases from colon carcinoma. *J Nucl Med* 1982;23: 1133–1137.
7. Messa C, Choi Y, Hoh CK, et al. Quantification of glucose utilization in liver metastases: parametric imaging of FDG uptake with PET. *J Comput Assist Tomogr* 1992;16:684–689.
8. Kubota K, Matsuzawa T, Fujiwara T, et al. Differential diagnosis of lung tumor with positron emission tomography: a prospective study. *J Nucl Med* 1990;31:1927–1932.
9. Strauss LG, Clorius JH, Schlag P, et al. Recurrence of colorectal tumors: PET evaluation. *Radiology* 1989;170:329–332.
10. Minn H, Aitasalo K, Happonen RP. Detection of cancer recurrence in irradiated mandible using positron emission tomography. *Eur Arch Otorhinolaryngol* 1993;250: 312–315.
11. Di Chiro G. Positron emission tomography using [^{18}F] fluorodeoxyglucose in brain tumors: a powerful diagnostic and prognostic tool. *Invest Radiol* 1987;22:360–371.
12. Okazumi S, Isono K, Enomoto K, et al. Evaluation of liver tumors using fluorine-18-fluorodeoxyglucose PET: characterization of tumor and assessment of effect of treatment. *J Nucl Med* 1992;33:333–339.
13. Hawkins RA, Choi Y, Huang S-C, Messa C, Hoh CK, Phelps ME. Quantitating tumor glucose metabolism with FDG and PET. *J Nucl Med* 1992;33:339–344.
14. Haberkorn U, Strauss LG, Reisser CH, et al. Glucose uptake, perfusion and cell

proliferation in head and neck tumors: relation of positron emission tomography to flow cytometry. *J Nucl Med* 1991;32:1548–1555.
15. Hawkins RA, Hoh C, Dahlborn M, et al. PET cancer evaluations with FDG. *J Nucl Med* 1991;32:1555–1558.
16. Rege S, Maass A, Chaiken L, et al. Use of positron emission tomography with fluorodeoxyglucose in patients with extracranial head and neck cancers. *Cancer* 1994;73:3047–3058.
17. Minn H, Paul R, Ahonen A. Evaluation of treatment response to radiotherapy in head and neck cancer with fluorine-18-fluorodeoxyglucose. *J Nucl Med* 1988;29:1521–1525.
18. Abe Y, Matsuzawa T, Fujiwara T, et al. Clinical assessment of therapeutic effects on cancer using ^{18}F-2-fluoro-2-deoxy-D-glucose and positron emission tomography: preliminary study of lung cancer. *Int J Radiat Oncol Biol Phys* 1990;19:1005–1010.
19. Haberkorn U, Strauss LG, Dimitrakopoulou A, et al. PET studies of fluorodeoxyglucose metabolism in patients with recurrent colorectal tumors receiving radiotherapy. *J Nucl Med* 1991;32:1485–1490.
20. Okada J, Oonishi H, Yoshikawa K, et al. FDG-PET for the evaluation of tumor viability after anticancer therapy. *Ann Nucl Med* 1994;8:109–113.
21. Mogard J, Kihlström L, Ericson K, Karlsson B, Guo WY, Stone-Elander S. Recurrent tumor versus radiation effects after gamma knife radiosurgery of intracerebral metastases: diagnosis with PET-FDG. *J Comput Assist Tomogr* 1994;18:177–181.
22. Rege SD, Chaiken L, Hoh CK, et al. Change induced by radiation therapy in FDG uptake in normal and malignant structures of the head and neck: quantitation with PET. *Radiology* 1993;189:807–812.
23. Nagata Y, Yamamoto K, Hiraoka M, et al. Monitoring liver tumor therapy with ^{18}F-FDG positron emission tomography. *J Comput Assist Tomogr* 1990;14:370–374.
24. Abe Y, Matsuzawa T, Fujiwara T, et al. Assessment of radiotherapeutic effects on experimental tumors using ^{18}F-2-fluoro-2-deoxy-D-glucose. *Eur J Nucl Med* 1986;12:325–328.
25. Kubota K, Ishiwata K, Kubota R, et al. Tracer feasibility for monitoring radiotherapy: a quadruple tracer study with fluorine-18-fluorodeoxyglucose or fluorine-18-fluorodeoxyuridine, L-[methyl-^{14}C] methionine, [6-^{3}H] thymidine, and gallium-67. *J Nucl Med* 1991;32:2118–2123.
26. Iosilevski G, Front D, Bettman L, Hardoff R, Ben-Arieh Y. Uptake of gallium-67-citrate and [2-^{3}H] deoxyglucose in the tumor model, following chemotherapy and radiotherapy. *J Nucl Med* 1985;26:278–282.
27. Minn H, Kangas L, Kellokumpu-Lehtinen, et al. Uptake of 2-fluoro-2-deoxy-D-[U-^{14}C]-glucose during chemotherapy in murine Lewis lung tumor. *Nucl Med Biol* 1992;19:55–63.
28. Hase M, Sako M, Hirota S. Experimental study of ferromagnetic induction heating combined with hepatic arterial embolization for treatment of liver tumors. *Nippon Act Radiol* 1990;50:1402–1414.
29. Shiue C-Y, Salvadori PA, Wolf AP, Fowler JS, MacGregor RR. A new improved synthesis of 2-deoxy-2-[^{18}F]fluoro-D-glucose from ^{18}F-labeled acetyl hypofluorite. *J Nucl Med* 1982;23:899–903.
30. Mitsumori M, Hiraoka M, Shibata T, et al. Development of intra-arterial hyperthermia using a dextran-magnetite complex. *Int J Hyperthermia* 1994;10:785–793.
31. Watanabe M, Uchida H, Okada H, et al. A high resolution PET for animal studies. *IEEE Trans Medical Imaging* 1992;11:577–580.
32. Patlak CS, Blasberg RG, Fenstermacher JD. Graphical evaluation of blood-to-brain transfer constants from multiple-time uptake data. *J Cereb Blood Flow Metab* 1983;3:1–7.
33. Patlak CS, Blasberg RG. Graphical evaluation of blood-to-brain transfer constants from multiple-time uptake data: generalizations. *J Cereb Blood Flow Metab* 1985;5:584–590.
34. Torizuka T, Tamaki N, Inokuma T, et al. Value of positron emission tomography using [^{18}F]fluorodeoxyglucose for monitoring hepatocellular carcinoma after interventional therapy. *J Nucl Med* 1994;35:1965–1969.
35. Rozental JM, Levine RL, Mehta MP, et al. Early changes in tumor metabolism after treatment: the effects of stereotactic radiotherapy. *Int J Radiat Oncol Biol Phys* 1991;20:1053–1060.
36. Kubota R, Yamada S, Kubota K, et al. Autoradiographic demonstration of [^{18}F]FDG distribution within mouse FM3A tumor tissue in vivo. *Kaku Igaku* 1992;29:1215–1221.
37. Kubota K, Matsuzawa T, Takahashi T, et al. Rapid and sensitive response of carbon-11-L-methionine tumor uptake to irradiation. *J Nucl Med* 1989;30:2012–2016.
38. Higashi K, Clavo AC, Wahl RL. Does FDG uptake measure proliferative activity of human cancer cells? In vitro comparison with DNA flow cytometry and tritiated thymidine uptake. *J Nucl Med* 1993;34:414–419.
39. Higashi K, Clavo AC, Wahl RL. In vitro assessment of 2-fluoro-2-deoxy-D-glucose, L-methionine and thymidine as agents to monitor the early response of a human adenocarcinoma cell line to radiotherapy. *J Nucl Med* 1993;34:773–779.
40. Hall EJ. *Radiobiology for the radiologist*, 4th ed. Philadelphia: JB Lippincott; 1994.

Accurate Measurement of Copper-67 in the Presence of Copper-64 Contaminant Using a Dose Calibrator

Gerald L. DeNardo, David L. Kukis, Sui Shen and Sally J. DeNardo
University of California Davis Medical Center, Sacramento, California

The use of ^{67}Cu-labeled antibodies for the treatment of cancer has advanced to the clinical trial phase. Quantitation of ^{67}Cu radiopharmaceuticals is complicated by the presence of the radioimpurity of ^{64}Cu in ^{67}Cu supplies. Here we report a method to assay ^{67}Cu and ^{64}Cu in a mixed sample with a commonly available instrument, the ionization chamber dose calibrator. **Methods:** The activities of ^{67}Cu and ^{64}Cu in a mixed sample can be calculated from a single-dose calibrator measurement. The calculation requires (1) instrument-specific response coefficients D_{67} and D_{64}, generated by gauging the instrument for the efficiency of measurement of ^{67}Cu and ^{64}Cu, and (2) a value for the ratio of ^{67}Cu to ^{64}Cu in the sample, routinely provided by major suppliers of ^{67}Cu. D_{67} and D_{64} were empirically determined by measuring samples containing known amounts of ^{67}Cu and ^{64}Cu. The samples were also assayed by gamma ray spectroscopy to verify the isotope ratios given by the suppliers. **Results:** This method generated accurate response coefficients. At the recommended dose calibrator setting for the measurement of ^{67}Cu, at which D_{67} = 1.0, the measurement for D_{67} with this method was 1.02 (± 0.04). Isotope ratios provided by the radionuclide suppliers were corroborated by gamma ray spectroscopy. **Conclusion:** A method is presented by which ^{67}Cu and ^{64}Cu in a mixed sample can be assayed using a dose calibrator. Although the derived numeric constants are only correct for a specific dose calibrator and setting, the method can be adapted for use with any dose calibrator.

Key Words: copper-67; radiocontaminant; dose calibrator
J Nucl Med 1996; 37:302–306

Radionuclides used in nuclear medicine, such as ^{67}Cu, ^{67}Ga, ^{99m}Tc, ^{111}In and ^{123}I, often contain radiocontaminants that complicate quantitation and increase the radiation dose absorbed by the patient (*1–3*). Strategies that use commonly available instruments such as a dose calibrator to assay contaminants in radiopharmaceuticals have been reported (*4–8*). We present a similar approach to measure ^{64}Cu radiocontamination in ^{67}Cu.

Due to its excellent physical and biochemical properties for radioimmunotherapy, ^{67}Cu is being actively investigated by several groups as a radioimmunotherapeutic agent (*9–13*). Copper-67 has a half-life of 62 hr, emits abundant beta particles and gamma rays, useful for therapy and pretherapy imaging studies, respectively, and has no known biological pathways for deposition in bone (*14,15*).

These studies have advanced to the clinical trial phase (*9,14*) using the chelating agent 1,4,8,11-tetraazacyclotetradecane-N,N′,N″,N‴-tetraacetic acid (TETA) as a carrier for ^{67}Cu (*16,17*). TETA binds ^{67}Cu rapidly, selectively, completely and

Received Dec. 16, 1994; revision accepted Jun. 7, 1995.
For correspondence or reprints contact: Gerald L. DeNardo, MD, Molecular Cancer Institute, 1508 Alhambra Blvd., Sacramento, CA 95816.